PROGRESS IN PHOTOVOLTAICS: RESEARCH AND APPLICATIONS
Prog. Photovolt. Res. Appl. 2007; **15**:375–386
Published online 5 February 2007 in Wiley InterScience (www.interscience.wiley.com) DOI: 10.1002/pip.744

Research

Effect of P-induced Gettering on Extended Defects in n-type Multicrystalline Silicon

M. Acciarri[1*,†], S. Binetti[1], A. Le Donne[1], S. Marchionna[1], M. Vimercati[1], J. Libal[2], R. Kopecek[2] and K. Wambach[3]
[1]*Department of Material Science, University of Milano-Bicocca, via Cozzi 53, I-20125 Milano, Italy*
[2]*University of Konstanz, Jakob-Burckhardt-Str. 29, D-78464 Konstanz, Germany*
[3]*Deutsche Solar AG, Alfred-Lange Str. 18, D-09599 Freiberg, Germany*

The electrical properties and the minority charge carrier recombination behaviour of grain boundaries (GBs) and intragrain dislocations in different n-type multicrystalline silicon (mc-Si) ingots were systematically studied through microwave-detected PhotoConductance Decay (μW-PCD), Electron Beam Induced Current (EBIC) and PhotoLuminescence (PL) spectroscopy on as-grown samples and on samples submitted to P-diffusion step. It was confirmed that the overall quality of n-type mc-Si is high, indicating that n-type-Si is a valid source for photovoltaic applications. As expected, the average lifetime increases after the P-diffusion process, which induces impurity gettering effects at the external surfaces, like in the case of p-type samples, but an evident local increase of electrical activity of some GBs after that process was also observed using the EBIC mapping technique. Apparently, a redistribution of impurities occurs at the processing temperature and impurities are captured at the deepest sinks. In fact, while all GBs act as heterogeneous segregation/precipitation sites, some of them will compete with the external surfaces sinks, partly vanishing the effect of P-gettering. Last but not least, it was experimentally demonstrated that the average lifetime values measured with the μW-PCD technique well correlate with the recombination activity of GBs measured with the EBIC technique, showing the extreme importance of GBs on the effective lifetime of this material.
Copyright © 2007 John Wiley & Sons, Ltd.

KEY WORDS: multicrystalline silicon; solar cells; gettering; lifetime; EBIC

Received 30 August 2006; Revised 17 November 2006

INTRODUCTION

It is well known that the directionally solidified (DS) multicrystalline silicon (mc-Si) has become a dominant material in the fast growing PV market for solar cells because of its cost-effectiveness and excellent electronic properties.

* Correspondence to: M. Acciarri, Department of Material Science, University of Milano-Bicocca, via Cozzi 53, I-20125 Milano, Italy.
† E-mail: maurizio.acciarri@unimib.it

WILEY InterScience® DISCOVER SOMETHING GREAT

Copyright © 2007 John Wiley & Sons, Ltd.

Nowadays commercial p-type mc-Si based solar cells achieve solar conversion efficiencies in the range of 15–16% with industrial standard processes, up to 17% with standard screen printing processes[1] and above 20% with more sophisticated solar cell designs.[2–4]

Recently, n-type mc-Si has attracted attention as a short term solution to the main current problem for the photovoltaic industry: the silicon supply. A partial solution not yet on the market, is in fact the use of the n-doped silicon waste available from the semiconductor industry.

For this purpose, in the last 3 years some works have been carried out on studies of the properties of n-type mc-Si and c-Si[5,6] and on the development and optimisation of a solar cell process for n-type mc-Si.[7] First results on solar cells based on n-type monocrystalline material using industrial processes have already shown excellent efficiencies exceeding 17%,[8] but some unknowns, concerning the specific role of certain impurities in a B-free material and that of their interaction with extended defects, still remain.

For this purpose, a systematic work has been carried out in our Laboratories on studies of the properties and defect features associated to microstructure disorder and to impurities contamination of different n-type mc-Si ingots grown by directional solidification (DS).

This paper deals therefore with two main topics. The first is an investigation of the effect of microstructural disorder on the optoelectronic properties of different n-type DS mc-Si ingots.

Since it has definitely been proven that in p-type mc-Si both the P-diffusion and the contact firing through SiN_x improve the overall carrier lifetime and quality of the material, due to external gettering and bulk hydrogenation respectively,[9,10] a further aim of this work was to check and to study in detail the effect the P-diffusion which is known to be the most effective for the improvement of electrical properties.[11,12]

As it is widely known that the recombination activity of extended defects strongly affects the electrical properties of the material and it is influenced by process-induced contamination, particular care was devoted to a local electrical characterisation of these defects.

EXPERIMENTAL DETAILS

Several n-type (P-, Sb- or As- doped) mc-Si ingots were grown from blended materials in the same industrial furnace and then were cut in wafers having a thickness ranging from 270 to 330 μm[7] and a resistivity between 0·2 and 1·8 Ohm cm. A p-type (B-doped) ingot was also grown in the same conditions, to be used for reference.

The characterisation was carried out on wafers coming from different heights of the ingots, that is from the bottom (solidified first) to the top (solidified last). For each part of the ingot (bottom, middle and top) a couple of nearby wafers with the same morphology were selected. One wafer for each couple was submitted to the P-diffusion step, according to the following procedure:

- Saw damage removal: 20 min CP4-etch (removal of 20 μm from each wafer side).
- P-diffusion step: 45 Ohm/sq $POCl_3$-diffusion ($T = 850°C$ approx. for 30 min).
- Removal of P-doped region: 30 min CP4-etch.

Table I shows details about the wafers characterised in this work (i.e. ingot type, dopant, positions and codes).

All wafers were characterised before and after the P-diffusion step as follows.

The interstitial oxygen [O_i] and substitutional carbon [C_s] content was determined by Fourier Transform InfraRed (FTIR) spectroscopy in the 400–4000 cm^{-1} range, at room temperature ASTM F1391·93; ASTM F1188 93a.

Using a microwave-detected PhotoConductance Decay (μW-PCD) Amecon Janus 300 Lifetime scanner system, spatially resolved lifetime maps were obtained. The Janus 300 uses a laser diode ($\lambda = 908$ nm) to inject the excess charge carriers, whose intensity has been chosen for all measurements so that the excess carrier density remained low compared to the dopant concentration in the respective silicon samples. An iodine–ethanol mixture[13] has been used for surface passivation of the wafers during the lifetime measurements.

To compare the properties of the n- and p-type materials, the arithmetic average diffusion lengths were calculated using the lifetime values obtained from the lifetime maps.

Copyright © 2007 John Wiley & Sons, Ltd.

Table I. Details of wafers (ingot codes, dopant type, resistivity and positions) characterised in this work

	Ingot code: #2	Ingot code: #4	Ingot code: #6	Ingot code: #B1	Height in the ingot (% from bottom)
	Dopant: Sb	Dopant: P	Dopant: Sb	Dopant: B	
As grown					
Wafer N° (resistivity)	#230 (0·2 Ωcm)	#348 (0·2 Ωcm)	#439 (0·5 Ωcm)	#331 (1·6 Ωcm)	80 Top
P-diff					
Wafer N° (resistivity)	#228 (0·2 Ωcm)	#342 (0·2 Ωcm)	#431 (0·5 Ωcm)	#329 (1·6 Ωcm)	80 Top
As grown					
Wafer N° (resistivity)	#119 (0·8 Ωcm)	#133 (0·36 Ωcm)	#245 (1·3 Ωcm)	#192 (1·7 Ωcm)	50 Middle
P-diff					
Wafer N° (resistivity)	#117 (0·8 Ωcm)	#136 (0·36 Ωcm)	#248 (1·3 Ωcm)	#168 (1·7 Ωcm)	50 Middle
As grown					
Wafer N° (resistivity)	#3 (1·3 Ωcm)	#1 (0·4 Ωcm)	#10 (2·6 Ωcm)	#14 (1·8 Ωcm)	5 Bottom
P-diff					
Wafer N° (resistivity)	#4 (1·3 Ωcm)	#4 (0·4 Ωcm)	#7 (2·6 Ωcm)	#6 (1·8 Ωcm)	5 Bottom

An approximate distance of the wafers from the bottom of the ingot is reported. All ingots were growth in block of 240 kg.

It is clear that these averages are computed without considering the heterogeneity of the material, in which both bulk defects and extended defects contribute differently to the carrier losses. In certain cases, also Surface PhotoVoltage (SPV) measurements were used for the determination of the diffusion length and the four-point probe technique (ASTM F43-93, 1996) for resistivity maps.

The local recombination activity of extended defects (dislocations and grain boundaries (GBs)) was studied by the Electron Beam Induced Current (EBIC) technique at room temperature. The EBIC measurements were carried out with a Vega TS5136 XM Tescan Scanning Electron Microscope equipped with an EBIC apparatus. The electron beam excitation was varied from 10 to 30 kV at a beam current kept always below 10 pA. A quantitative analysis of the recombination activity of extended defects was obtained using the EBIC contrast (C) defined by $C = (I_b - I_g)/I_b$ where I_b and I_g are the EBIC currents in the bulk and at the grain boundary (GB), respectively. In the case of our set-up, the minimum contrast significantly measurable has been estimated to be close to 0·2% on as-grown polished samples.

Before the EBIC measurements, the samples were mechanically and then chemically polished with CP4 ($HF:HNO_3:CH_3COOH = 3:5:3$ in volume ratio). Thereafter, Au or Al Schottky contacts were realised by evaporating the metal under vacuum conditions of about 10^{-8} Pa.

Some samples were also etched with a SCHIMMEL solution (1 g CrO_3/20 ml HF 48%/10 ml H_2O) in order to highlight the presence of crystallographic defects, detected and counted both by optical and ELectron MIcroscopy (ELMI).

Photoluminescence (PL) measurements were also carried out to get supplementary information on radiative recombination processes occurring under illumination: the PL spectra were recorded at 14 K with a spectral resolution of 6·6 nm, using an InGaAs detector and a quantum well laser ($\lambda = 805$ nm) as excitation source.

EXPERIMENTAL RESULTS

Oxygen and carbon concentration

In order to evaluate a possible role of native impurities on the overall behaviour of n-type ingots, the profiles of concentration of $[O_i]$ and $[C_s]$ were measured using the FTIR technique.

Figure 1 displays a typical concentration profile of the two impurities along the growth direction. The oxygen and carbon distribution along the growth direction is congruent with the segregation coefficient of these impurities.[14] It should be remarked that the O_i concentration ranges between 10 and less that 1 ppma, and that the carbon concentration exceeds that of oxygen in the major part of the ingot. The fact that in the top part of the

Copyright © 2007 John Wiley & Sons, Ltd.

DOI: 10.1002/pip

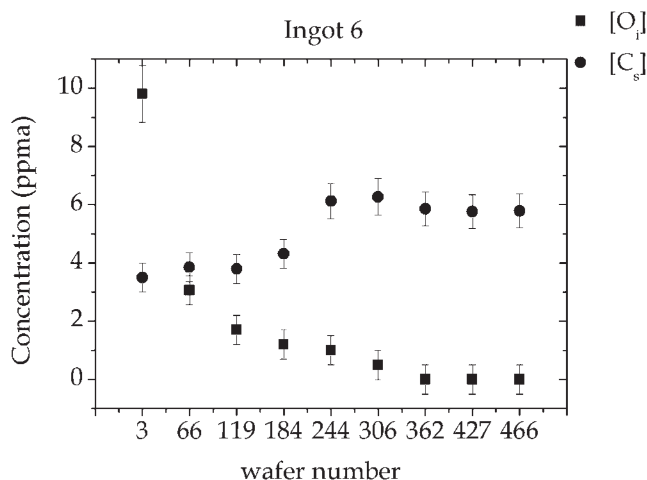

Figure 1. A typical oxygen and carbon distribution in DS's n-type ingot

ingot the carbon concentration remains almost constant suggests the occurring of SiC precipitation, due to C supersaturation.[15]

Minority carriers properties from spatially resolved lifetime measurements

In order to understand the gettering effect of the P-diffusion process on n-type samples, the lifetime of the samples under investigation has been measured before and after this solar step process by spatially resolved lifetime measurements.

We report in Figure 2, as a typical example, two lifetime maps carried out on a $5 \times 5\,\mathrm{cm}^2$ section of a wafer coming from the middle position of the ingot 2 (Sb-doped) before (Figure 2a) and after the P-diffusion process, followed by the removal of the doped region (Figure 2b), respectively. The average lifetime increases after the P-diffusion due to the gettering process, but regions of low lifetime are still present. This behaviour does not depend on the dopant used (Sb or P) and has been observed also in the p-type reference ingot.

The increase of the average lifetime after P step is clearly demonstrated in Figure 3, where the average diffusion lengths are reported for all the ingots considered in this work. In particular, it could be observed that the higher relative increase was obtained for the bottom and top parts of the ingots. This behaviour can be explained taking into account that the gettering effect should become more evident where a higher metallic contamination is present, as occurs in the top and bottom part of such ingots.

In order to understand why low lifetime regions remain after the P-diffusion step, we performed local characterisations of such regions, indicated in the following as 'bad zones'. For comparison purposes, also sample sections coming from high lifetime regions and denoted as 'good zones' have been analysed.

About the radiative recombination processes occurring in as-grown and gettered samples

The knowledge of the defect related radiative recombination processes is of customary importance because it allows the identification of specific minority carrier recombination steps and of their role on the overall lifetime losses. In addition, by the measurement of the intensity of the Free Exciton (FE) emission the quality of the sample can be judged.[16]

The PL spectra collected in 'good zones' of the as-grown ingots present high FE emission intensity, in agreement with the high lifetime values measured on the same samples and confirming the overall good quality of the as-grown ingots. Furthermore, they present as well, quite systematically, the D1–D4 peaks associated to dislocations,[17] and an additional peak around 1·04 eV (see Figure 4).

Copyright © 2007 John Wiley & Sons, Ltd.

DOI: 10.1002/pip

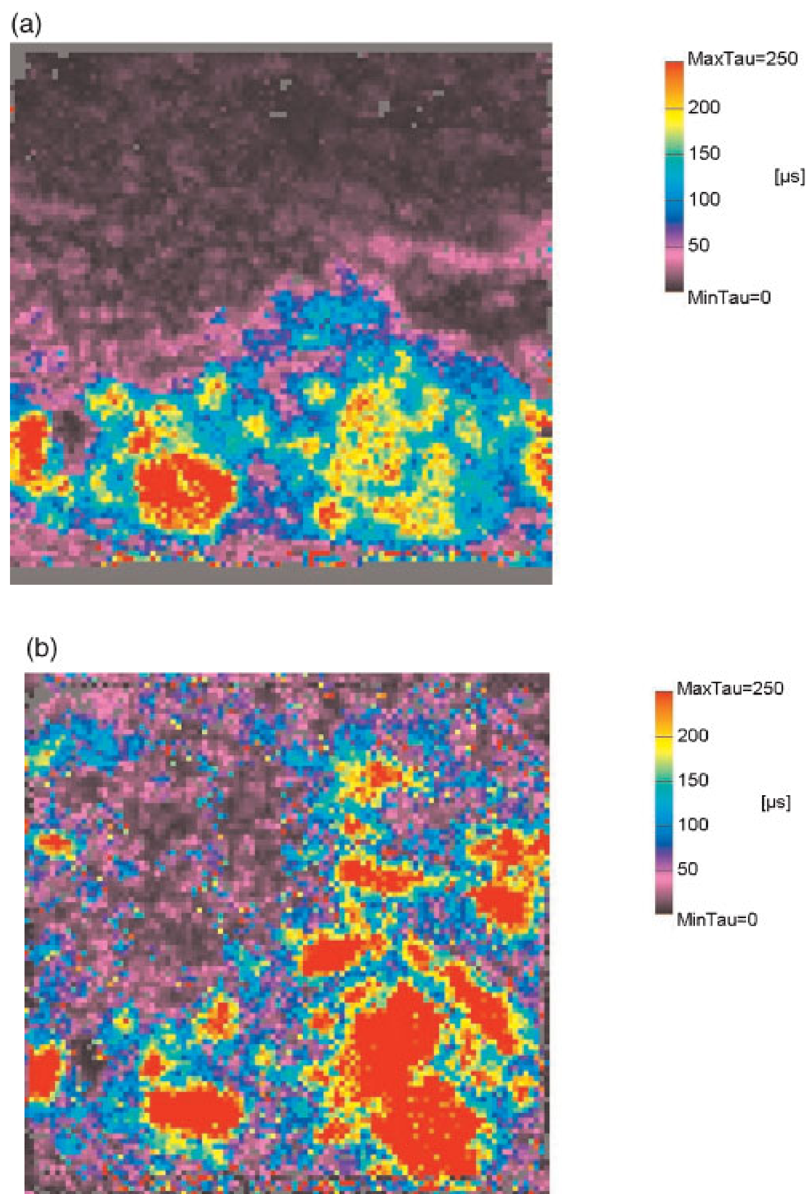

Figure 2. Lifetime μW-PCD maps of a wafer coming from the middle part of ingot 2 before (a) and after (b) the $POCl_3$ process step. Size of the measured wafers: $5 \times 5\,cm^2$

According to[18] and,[19] this emission falls in the region related to self-interstitial clusters, and according to our experience it is a typical PL signature of mc-Si.

Taking into account the energy position of the last emission, one or two shallow levels should be involved, which should play, therefore, a negligible role in lifetime losses.

It is to be noted, eventually, that mainly in the bottom parts of the as-grown ingots, where the oxygen content takes the largest value, the PL spectra present emission bands at 0·8 eV, which could be attributed to nuclei and precipitates of silicon dioxide.[20]

The effect of P-gettering detected by PL measurements is a systematic increase of the FE emission, which calls for an increase of the average lifetime, but in some bad zones also an increase of the PL emission associated to oxide precipitates, which calls for a process-temperature induced oxide precipitation.

Copyright © 2007 John Wiley & Sons, Ltd.

DOI: 10.1002/pip

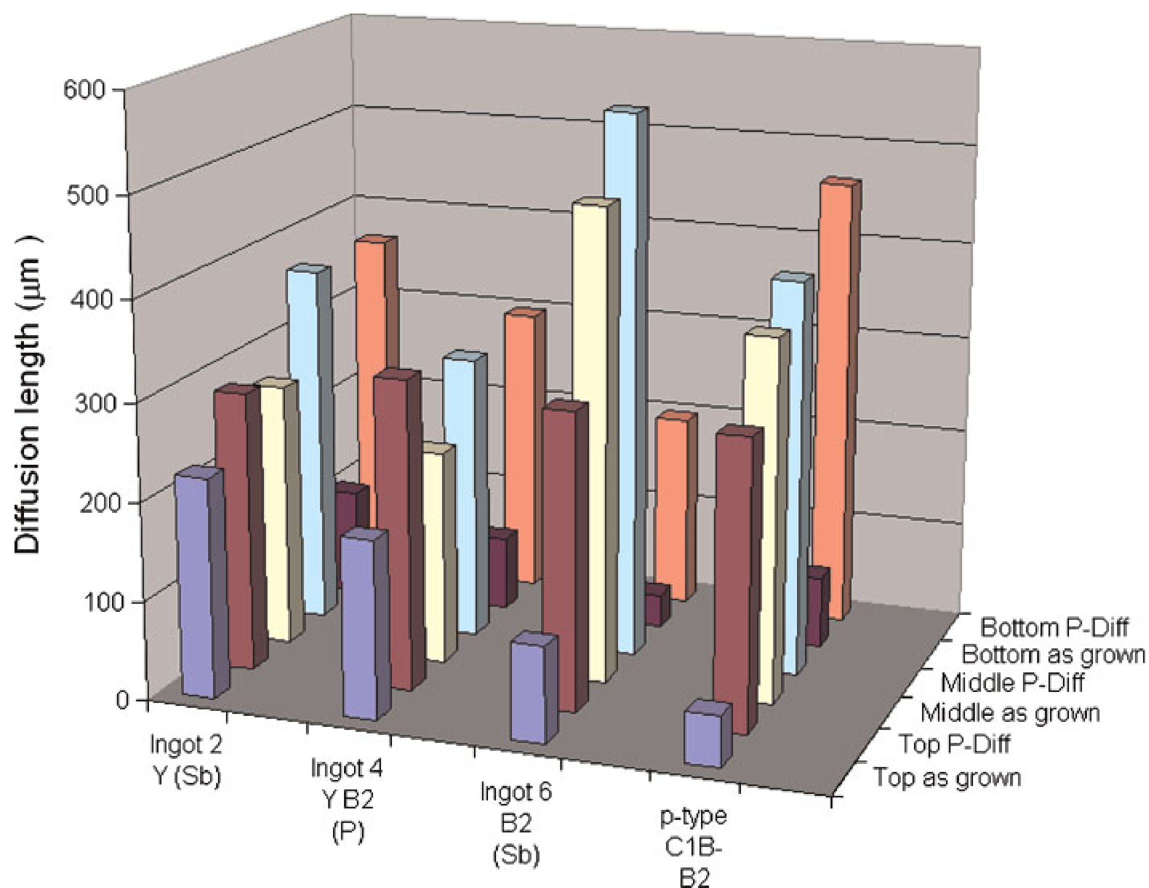

Figure 3. Average diffusion length calculated using the lifetime data obtained by µW-PCD for the wafers from different ingots before and after the P-gettering

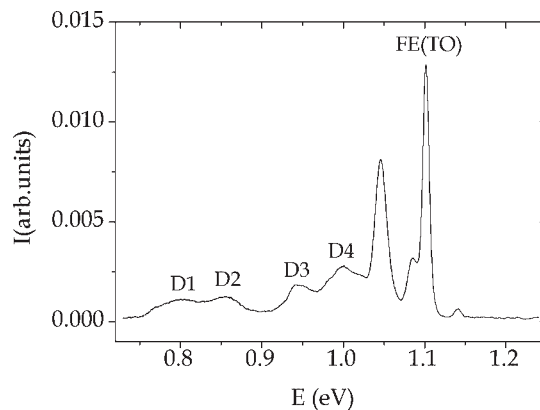

Figure 4. Typical PL spectrum collected for 'good zone' samples ($T = 12$ K, power density: 6 W/cm^2, spot size: 1 mm^2). The dislocation related bands are indicated with the classic notations [D1 (0·81 eV), D2 (0·87 eV), D3 (0·94), D4 (0·99 eV)]

Copyright © 2007 John Wiley & Sons, Ltd.

DOI: 10.1002/pip

About the non-radiative recombination processes at extended defects

In order to correlate the electrical activity of extended defects with the average electrical and optical properties of the samples investigated in this work, EBIC maps were collected on wafers coming from different ingot positions. In particular, whenever possible, the same GB was characterised in different sections of the ingot, before and after the P-diffusion step.

Figure 5 reports a typical EBIC map collected in a 'good zone' of an as-grown sample coming from the middle position of the Sb-doped ingot 6. Electrically active GBs are clearly visible, on which the EBIC contrast was quantitatively determined with the largest spatial resolution possible. Almost in the case of all the as-grown samples studied in this work, the EBIC contrast rarely exceeds 10%. Higher values, of the order of 20–40%, have

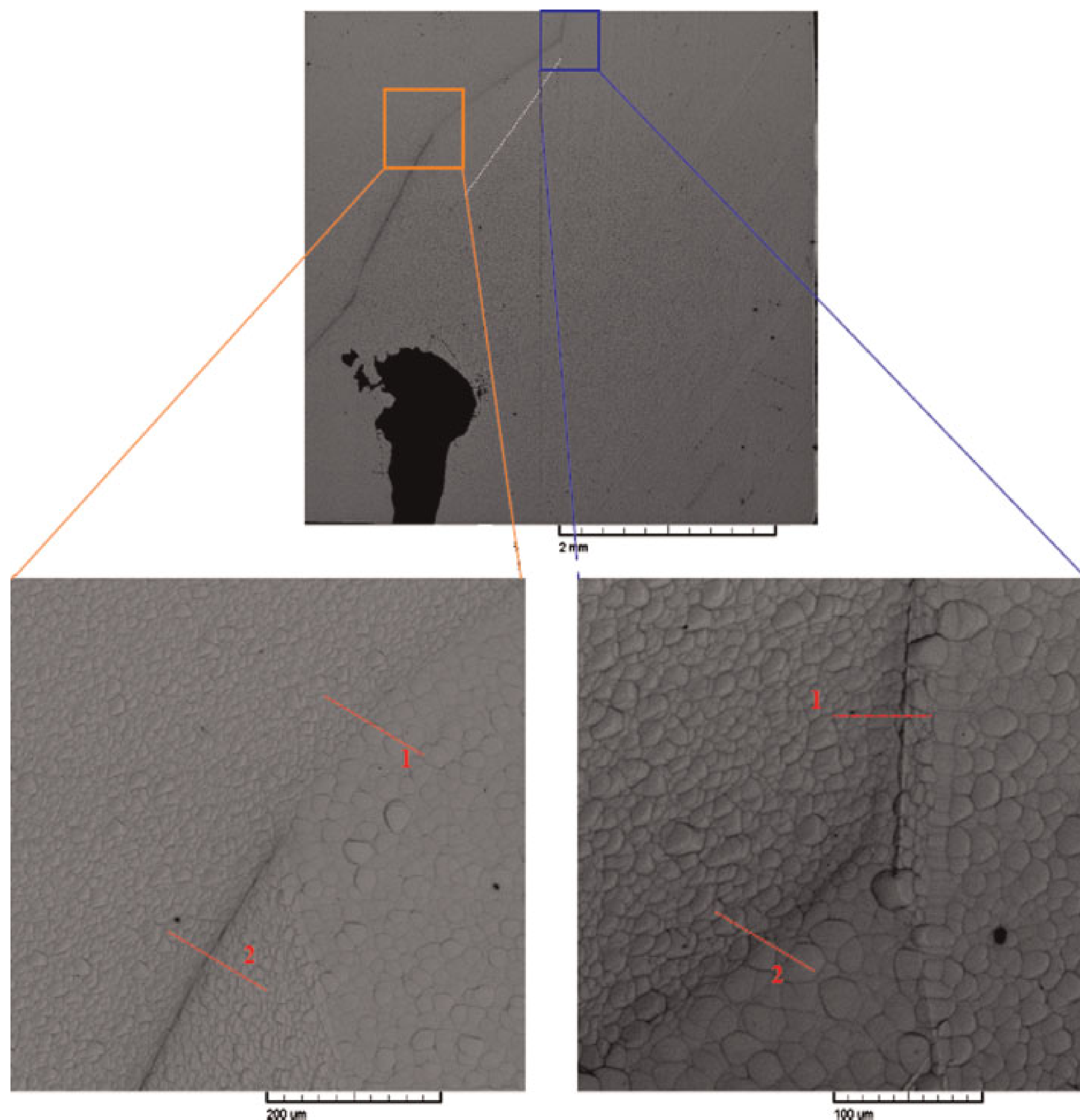

Figure 5. EBIC map of good zones for a middle wafer of the Sb doped ingot 6. In the magnification the measured EBIC contrasts are reported. The big dark spot in the first picture is the contact while the small dark spots are due to dust on the diode surface

Copyright © 2007 John Wiley & Sons, Ltd.

DOI: 10.1002/pip

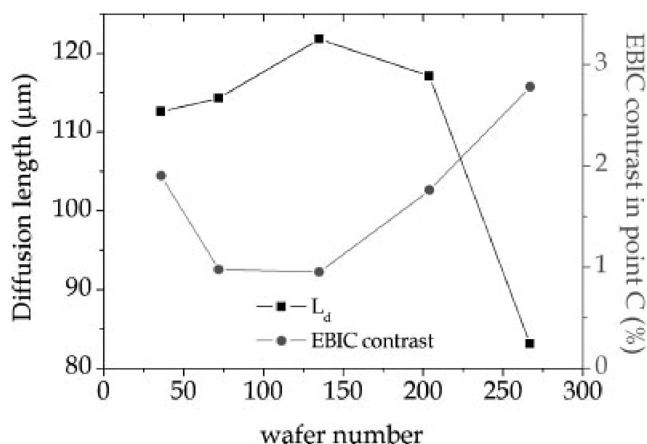

Figure 6. Comparison between the diffusion length values (left side) and the EBIC contrast (right side) versus wafer numbers

been detected only in the top and bottom parts of the ingots, while in the samples coming from the middle part of the ingot high contrast values have been observed only in the 'bad zones'.

Figure 6 reports the contrast profile for one single GB running along the ingot. In the same Figure the average diffusion length values measured in the same regions are reported.

One could observe that a good correlation exists between the GB contrast and the average diffusion length, which both show a strong degradation towards the top of the ingot.

As it was emphasised before, during the crystal growth metallic impurities tend to segregate towards the top of the ingot, due to their very low segregation coefficients. The results reported in Figure 6 show therefore that the increase of the metallic impurity concentration on the top of the ingot enhances the recombination activity of the GB while decreasing the average lifetime.

Therefore, the decrease of the average lifetime is associated both to the recombination effect of a concentrated solution of impurities and to the increase of the recombination activity of GBs, which behave as sinks for metallic impurities.

After the P-diffusion process (Figure 7) a significant increase in the contrasts was observed for some GBs, as is the case of the GB shown in Figure 5. An increase of the GB contrast, even when the average lifetime is enhanced with respect to that of the corresponding as-grown samples, is an evidence that during the $POCl_3$ process a segregation/precipitation of impurities at extended defects occurs, as already observed by Istratov *et al*.[21]

It is important to note, eventually, that EBIC analysis do not show the presence of electrically active dislocations both in the as grown and the P-diffused samples, also in regions where a high density of dislocations has been revealed by chemical etching. As an example, Figure 8 shows a selected zone of an Sb doped wafer before and after the $POCl_3$ process step. Here, the increased activity of the extended defects (GBs) is again evident, while no active dislocations are detected, despite their high density, as shown in Figure 9.

DISCUSSION

One of the most relevant results of the present investigation is about the correlation between the lifetime decrease and the GBs contrast increase, showing that the GBs are the most detrimental extended defects in mc-Si.

This is confirmed by the absence of EBIC contrast associated to dislocations at room temperature, indicating a low level of metallic decoration of dislocation, according to Kveder's theory.[22]

Both the GBs activity and the lifetime evolve dramatically in correspondence of the top part of the ingot, with a behaviour which is very close to that observed in p-type silicon. This behaviour has been explained in

Copyright © 2007 John Wiley & Sons, Ltd.

DOI: 10.1002/pip

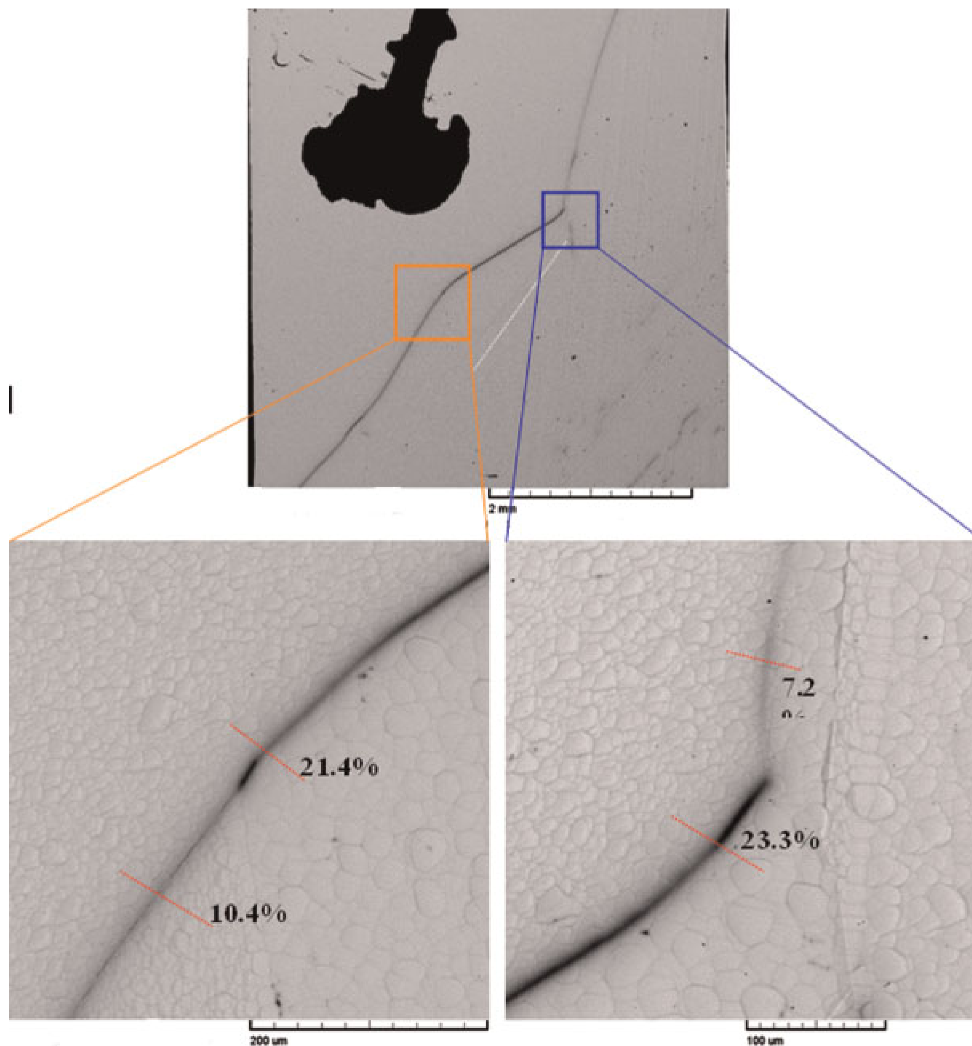

Figure 7. EBIC map of 'good zones' for a middle wafer of the Sb doped ingot 6 after the $POCl_3$ process step. In the magnification the measured EBIC contrasts are reported. The big dark spot in the first picture is the contact while the small dark spots are due to dust on the diode surface

literature[23–25] as an effect of a metallic impurity, most probably iron, which is a major contaminant of the silicon nitride liner of the quartz crucible and which is therefore expected to be dissolved in the Si matrix.

Concerning the effect of P-gettering process, the results of this work show that there is not a substantial difference between the beneficial effects arising on p-type and n-type mc-Si and such a result could not be judged by *a priori* evaluation.

It is therefore demonstrated that P-gettering might be employed in n-type ingots as a common solar cell production practice.

EBIC analyses have however shown that a competition exists between the surface gettering sites induced by P-diffusion and (specific) GBs. Several GBs contrast maps, in fact, show an evident increase of local electrical activity after the P-diffusion process. These regions, therefore, not only do not respond to external gettering procedures, but become decorated with impurities during the (high temperature) $POCl_3$ process.

During the high temperature $POCl_3$ process impurities dissolved in the grains are, in fact, driven towards GBs, dislocations and external gettering sites by chemical potential gradients and strain fields.[26,27] Our present results

Copyright © 2007 John Wiley & Sons, Ltd.

DOI: 10.1002/pip

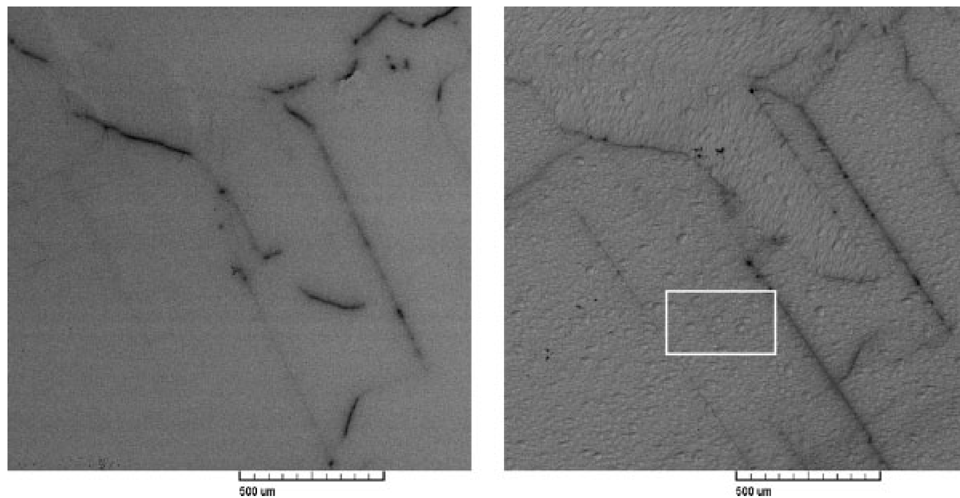

Figure 8. EBIC maps of a selected zone of an Sb doped wafer before (left) and after (right) the $POCl_3$ process step. The square in the figure indicates the zone magnified by the optical microscope and reported in Figure 9

show that at least a fraction of impurities are trapped at GBs, where impurities find a stable thermodynamic configuration, making the external gettering only partially efficient.

When local supersaturation conditions occur, during the cooling down stage, also precipitation processes might occur. The dark spot clearly visible in EBIC maps could be therefore related to cluster of precipitates of a second phases, decorating GBs. Even if we do not have a direct experimental information about the nature of these precipitates, we can infer, from recent literature results on materials grown with the same process,[21] that they consist of nanoprecipitates of silicides and oxides, depending on the metal species involved. We cannot however exclude, as carbon determination analysis has indicated, the presence of silicon carbide precipitates.

It could be furthermore argued that this impurity redistribution process is activated by the high temperature associated to the $POCl_3$ process. This has definitively been proved by carrying out thermal annealing experiments (850°C for 30 min) on the same material, which showed an increase of local electrical activity of some GB (see Figure 10). As can be inferred from the Figure 10, we have confirmed that the strength of the internal gettering depends on GBs structure, as already demonstrated by Chen *et al*.[28]

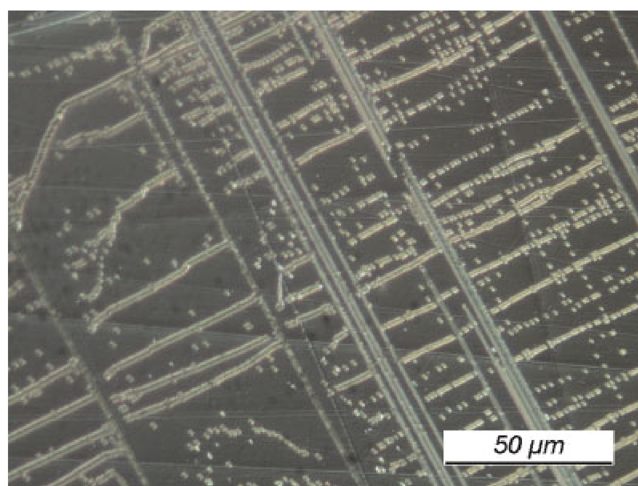

Figure 9. Optical image of the selected zone marked in Figure 8 after Schimmel etching. The etch pits clearly indicate a high density of emerging dislocations

Copyright © 2007 John Wiley & Sons, Ltd.

DOI: 10.1002/pip

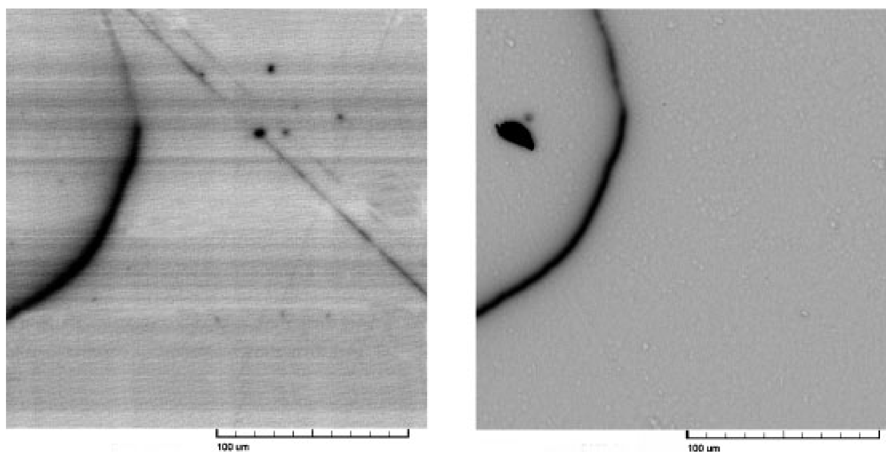

Figure 10. EBIC maps of a n-type samples before (left) and after (right) the heat treatment at 850°C for 30 min

CONCLUSIONS

We have shown that during the P-diffusion step in n-type silicon an impurity redistribution takes place and that both an internal and an external gettering process occurs, with GBs acting as secondary gettering sinks for impurities. As we have demonstrated that this impurity redistribution process is thermally activated, this result may be useful for a future optimisation of the solar cell process, taking particular attention to the time and annealing temperature.

Despite the intriguing effects of impurity segregation and precipitation at GBs, and the associated increase of their electrical activity, we have confirmed that n-type feedstocks are compatible with high quality mc-Si, possibly better than that of the p-type materials, confirming that n-type-Si is a valid resource for photovoltaic applications.

Acknowledgements

The authors warmly thank Professor Sergio Pizzini for his contributions to fruitful discussions on the argument. This work was supported by the European Commission within both the NESSI project (contract number ENK6-CT2002-00660) and the FOXY project (contract number 019811).

REFERENCES

1. Weeber AW, Granek FJ, Hoornstra J, Koppes M, Kossen EJ, Rieffe HC, Romijn IG, Tool CJJ. *Proceedings of the 20th European Photovoltaic Solar Energy Conference*, 2005 Barcelona (Spain).
2. McCann M, Raabe B, Jooss W, Kopecek R, Fath P. *Proceedings of 4th World Conference on Photovoltaic Energy Conversion*—May 7–12, 2006 Waikoloa, Hawaii, USA.
3. Schultz O, Glunz SW, Willeke GP. *Multicrystalline* silicon solar cells exceeding 20% efficiency. *Progress in Photovoltaics: Research and Applications* 2004; **12**: 553–558.
4. Brendle W, Nguyen VX, Grohe A, Schneiderlochner E, Rau U, Palfinger G, Werner JH. 20.5% efficient silicon solar cell with a low temperature rear side process using laser-fired contacts. *Progress in Photovoltaics: Research and Applications* 2006; **14**: 653–662.
5. Martinuzzi S, Palais O, Ostapenko S. Scanning techniques applied to the characterisation of P and N type multi-crystalline silicon. *Material Science in Semiconductor Processing* 2006; **9**: 230–235.
6. Geerlings LJ, Macdonald D. Base doping and recombination activity of impurities in crystalline silicon solar cells. *Progress in Photovoltaics: Research and Applications* 2004; **12**: 309–316.

Copyright © 2007 John Wiley & Sons, Ltd.

DOI: 10.1002/pip

7. Kopecek R, Libal J, Buck T, Peter K,Wambach K, Acciarri M, Binetti S, Geerligs LJ, Fath P. *Proceedings of Conference Record of the 31st IEEE Photovoltaic Specialists Conference* 2005.
8. Buck T, Kopecek R, Libal J, Petres R, Peter K, Röver I, Wambach K, Geerligs LJ, Wefringhaus E, Fath P. *Proceedings of 4th World Conference on Photovoltaic Energy Conversion*—May 7–12, 2006 Waikoloa, Hawaii, USA.
9. Perichaud I. Gettering of impurities in solar silicon. *Solar Energy Materials and Solar Cells* 2002; **72**: 315–326.
10. Kruger O, Seifert W, Kittler M. Vyvenko extension of hydrogen passivation of intragrain defects and grain boundaries in cast multicrystalline silicon. *Physica Status Solidi (b)* 2000; **222**: 367–378.
11. Manashanden P, Geerligs LJ. Improved phosphorous gettering of multicrystalline silicon. *Solar Energy Materials and Solar* 2006; **90**: 998–1012.
12. Bentzen A, Holt A, Kopecek R, Stokkan G, Christensen JS, Svensson BG. Gettring of transition metal impurities during phosphorus emitter diffusion in multicrystalline silicon solar cell processing. *Journal of Applied Physics* 2006; **99**: 093509-1–093509-6.
13. Horanyi TS, Pavelka T, Tutto T. In situ bulk lifetime measurement on silicon with a chemically passivated surface. *Applied Surface Science* 1993; **63**: 306.
14. Zulehner W, Huber D. *Czochralski Grown Silicon, Crystals Growth Properties and Application Vol. 8 Silicon Chemical Etching*, Grabmaier J (ed.). Springer: New York, 1982.
15. Newman R. *Materials Research Society Symposium Proceedings* 1986; **59**: 403.
16. Tarasov I, Ostapenko S, Haessler C, Reisner EU. Spatially resolved defect diagnostics in multicrystalline silicon for solar cells. *Materials Science and Engineering B* 2000; **71**: 51–55.
17. Drozdov NA, Patrin AA, Tkachev VD. Recombination radiation on dislocations in silicon. *Pis'ma V Zhurnal Tekhnicheskoi Fiziki* 1976; **23**: 651–653. [Soviet Physics JETP Letters 1976; **23**: 597].
18. Nakamura M, Murakami S. Evolution of photoluminescence defect clusters in proton- and copper-implanted silicon crystals during annealing. *Journal of Applied Physics* 2003; **94**: 3075–3081.
19. Giri PK, Coffa S, Rimini E. Evidence for small interstitial clusters as the origin of photoluminescence W band in ion-implanted silicon. *Applied Physics Letters* 2001; **78**: 291–293.
20. Leoni E, Martinelli L, Binetti S, Borionetti G, Pizzini S. The origin of photoluminescence from oxygen precipitates nucleated at low temperature in semiconductor silicon. *Journal of the Electrochemical Society* 2004; **151**: G866–G869.
21. Istratov AA, Buonassisi T, McDonald RJ, Smith AR, Schinder R, Rand JA, Kalejs JP, Weber ER. Metal content of multicrystalline silicon for solar cells and its impact on minority carrier diffusion length. *Journal of Applied Physics* 2003; **94**: 6552–6559.
22. Kveder V, Kittler M, Schroter W. Metal content of multicrystalline silicon for solar cells and its impact on minority carrier diffusion length. *Physical Review B* 2001; **63**: 115208-1–115208-11.
23. Binetti S, Acciarri M, Savigni C, Brianza A, Pizzini S, Musinu A. Effect of nitrogen contamination by crucible encapsulation on polycrystalline silicon material quality. *Materials Science and Engineering B* 1996; **36**: 68–70.
24. Macdonald D, Cuevas A, Kinomura A, Nakano Y, Geerligs LJ. Transition-metal profiles in a multicrystalline silicon ingot. *Journal of Applied Physics* 2005; **97**: 033523–033530.
25. Rossberg M, Naumann M, Irmscher K, Juda U, Ludge A, Ghosh M, Muller A. Investigation of defects in the edge region of multicrystalline solar silicon ingots. *Solid State Phenomena* 2005; **108–109**: 531–538.
26. Pizzini S. Chemistry and physics of defect interaction in semiconductors. *Solid State Phenomena* 2002; **85–86**: 1–66.
27. Istratov AA, Huber W, Weber ER. Experimental evidence for the presence of segregation and relaxation gettering of iron in polycrystalline silicon layers on silicon. *Applied Physics Letters* 2004; **85**: 4472–4474.
28. Chen J, Sekiguci T, Yang D, Yin F, Kido K, Tsurekawa S. Electron-beam-induced current study of grain boundaries in multicrystalline silicon. *Journal of Applied Physics* 2004; **96**: 5490–5495.

Copyright © 2007 John Wiley & Sons, Ltd.

DOI: 10.1002/pip